PHYSICAL REVIEW D **78,** 102002 (2008)

Spacetime encodings. II. Pictures of integrability

Jeandrew Brink

Theoretical Astrophysics, California Institute of Technology, Pasadena, California 91103, USA

(Received 8 July 2008; published 5 November 2008)

I visually explore the features of geodesic orbits in arbitrary stationary axisymmetric vacuum (SAV) spacetimes that are constructed from a complex Ernst potential. Some of the geometric features of integrable and chaotic orbits are highlighted. The geodesic problem for these SAV spacetimes is rewritten as a 2 degree of freedom problem and the connection between current ideas in dynamical systems and the study of two manifolds sought. The relationship between the Hamilton-Jacobi equations, canonical transformations, constants of motion, and Killing tensors are commented on. Wherever possible I illustrate the concepts by means of examples from general relativity. This investigation is designed to build the readers' intuition about how integrability arises, and to summarize some of the known facts about 2 degree of freedom systems. Evidence is given, in the form of an orbit-crossing structure, that geodesics in SAV spacetimes might admit a fourth constant of motion that is quartic in momentum (by contrast with Kerr spacetime, where Carter's fourth constant is quadratic).

DOI: 10.1103/PhysRevD.78.102002 PACS numbers: 04.80.Cc, 04.20.Jb, 04.30.Db

I. INTRODUCTION

The Carter constant associated with a Kerr spacetime plays a crucial role in current LIGO (Laser Interferometer Gravitational Wave Observatory) and LISA (Laser Interferometer Space Antenna) extreme and intermediate mass ratio inspiral (EMRI/ IMRI) waveform calculations. Its generalization to arbitrary stationary axisymmetric vacuum (SAV) spacetimes, could lead to an algorithm to map spacetimes around a compact object described by a general set of multipole moments; see [1] and paper I of this series [2]. Such an algorithm may provide a method of determining the nature of compact objects by asymptotically observing gravitational and electromagnetic radiation from an EMRI or IMRI.

The geodesic problem in Kerr spacetime is completely solved by the specification of four isolating integrals or constants of motion, namely, rest mass, energy, axial angular momentum, and the Carter constant (μ, E, L_z, Q). The generalization of the first three constants of motion, namely, (μ, E, L_z) to SAV spacetimes is trivial. These constants result from the absence of an explicit dependence of the Lagrangian on proper time, coordinate time, and the axial angular coordinate, respectively (τ, t, ϕ). The meaning of the fourth constant Q, first discovered by Brandon Carter by separation of the Hamilton-Jacobi equations (HJEs) [3,4] is a little more obscure. It is this fourth constant that allows the reduction of the geodesic equations to first order quadratures, and the complete solution of the geodesic problem. The geometric interpretation of this fourth constant and the conditions for its existence are explored in this and subsequent papers in this series [5,6].

The present paper visually characterizes the geodesics in some of the axisymmetric spacetimes that are generated from an Ernst potential. In particular, the Manko-Novikov [7–9] and Zipoy-Voorhees metrics [10,11] are considered. The geodesic problem is formulated as a 2 degree of freedom (2-DOF) problem in dynamical systems. Ideas from the field of integrable systems are collated and introduced by means of a series of visual examples. For historic purposes, the role of the HJE is put in context. Possible tests for integrability are addressed. The concepts of phase and energy space are introduced and illustrated by means of an example. The role and possible forms of the additional invariant are explored and a geometric interpretation of Killing tensors given.

Finally, some of the frustrations and computational difficulties when dealing with 2-DOF Hamiltonians are mentioned, and the implications of the numerical experiments in SAV spacetimes for the existence of a generalized Carter constant are described.

II. EQUATIONS OF MOTION

I begin with the general SAV spacetime line element of the form

$$ds^2 = k^2 e^{-2\psi}[e^{2\gamma}(d\rho^2 + dz^2) + R^2 d\phi^2] - e^{2\psi}(dt - \omega d\phi)^2, \tag{1}$$

where ψ, γ, ω, and R are functions of ρ and z, and k is a real constant. The vacuum field equations relate these functions to solutions of the Ernst equation for the complex potential $\mathcal{E}$,

$$\Re(\mathcal{E})\bar{\nabla}^2\mathcal{E} = \bar{\nabla}\mathcal{E}\cdot\bar{\nabla}\mathcal{E}, \tag{2}$$

where $\bar{\nabla}^2 = \partial_{\rho\rho} + \frac{1}{\rho}\partial_\rho + \partial_{zz}$, $\bar{\nabla} = (\partial_\rho, \partial_z)$, and the dot is the flat-space inner product. In particular, the function $e^{2\psi} = \Re(\mathcal{E})$ denotes the real part of the potential. The functions γ and ω can be obtained by means of line integrals of the potential once it is known. A gauge freedom in the form of the harmonic function R obeying $R_{zz} + R_{\rho\rho} = 0$ exists in this metric. Often this freedom is used to

set $R = \rho$, however, for the sake of later comparison with solution generation techniques, I shall retain this generality.

The Hamiltonian associated with geodesics of this metric is

$$\mathcal{H}(q, p) = \tfrac{1}{2} g^{\mu\nu} p_\mu p_\nu, \tag{3}$$

where, following the notation of Goldstein [12], $q = (\rho, z, \phi, t)$ are the generalized coordinates and $p = (p_\rho, p_z, p_\phi, p_t)$ are the conjugate momenta.

In order to write the equations of motion in compact form, I make use of the Poisson brackets. The Poisson bracket of two functions g and h with respect to the canonical variables is defined as

$$[g, h] = \sum_k \left(\frac{\partial g}{\partial q_k} \frac{\partial h}{\partial p_k} - \frac{\partial g}{\partial p_k} \frac{\partial h}{\partial q_k} \right). \tag{4}$$

The geodesic equations can now be expressed in first order form using Hamilton's equations, namely

$$\dot{q}_\mu = [q_\mu, \mathcal{H}], \qquad \dot{p}_\mu = [p_\mu, \mathcal{H}], \tag{5}$$

where the dot $\cdot$ indicates the total derivative with respect to proper time τ.

Using this notation it is immediately obvious that the absence of any explicit metric dependence on t and ϕ results in $\dot{p}_t = \dot{p}_\phi = 0$. By setting these quantities equal to the standard constants $p_t = -E$ and $p_\phi = L_z$, the study of geodesic motion in four-dimensional spacetime is reduced to the study of a 2-DOF dynamical system with an effective potential. The reduced Hamiltonian can be expressed as

$$H(\rho, z, p_\rho, p_z) = \frac{1}{2} \left(\frac{1}{V} (p_\rho^2 + p_z^2) - G \right), \tag{6}$$

where the two potentials V and G have been introduced to simplify notation, and are defined as

$$V(\rho, z) = k^2 e^{2\gamma - 2\psi}, \tag{7}$$

$$G(E, L_z, \rho, z) = -g^{AB} p_A p_B, \tag{8}$$

with A, B indicating the components t, ϕ, and let i, j range over ρ, z. The Hamiltonian constant $H = -1/2\mu^2$ fixes the sum of the squares of the conjugate momenta to

$$p_\rho^2 + p_z^2 = (G - \mu^2) V \equiv J(\rho, z, E, L, \mu^2), \tag{9}$$

and the equations of motion become

$$\dot{q}_i = \frac{p_i}{V}, \qquad \dot{p}_i = \frac{\partial_{q_i} J}{2V}. \tag{10}$$

Upon introducing the nonaffine parameter λ such that $V d\lambda = d\tau$, and letting $'$ indicate differentiation with respect to λ, the equations further simplify to

$$q_i' = p_i, \qquad p_i' = \tfrac{1}{2} \partial_{q_i} J. \tag{11}$$

The problem of finding a generalized Carter constant in SAV spacetimes can be expressed most generally as the hunt for a function $Q(\rho, z, p_\rho, p_z)$ distinct from the Hamiltonian $H(\rho, z, p_\rho, p_z)$, that remains constant along an orbit of the two-dimensional Hamiltonian H, i.e. a function such that $[Q, H] = 0$. Alternatively this can be stated as the study of the geodesics of the two manifold with metric g_J and associated "Jacobi" Hamiltonian H_J,

$$g_{Jij} = J \delta_{ij}, \qquad H_J = \frac{(p_\rho^2 + p_z^2)}{2J} = \frac{1}{2}. \tag{12}$$

A more general and rigorous treatment of these ideas is given in [13].

In general, for a generic two-dimensional Hamiltonian H_g, no such integral of motion Q_g exists and the Hamiltonian is chaotic. In most textbooks on dynamical systems completely integrable systems are given but brief mention [12,14,15]. Explicit examples are rare. A thorough review summarizing most of the known examples can be found at [16].

III. A FEW WORDS ABOUT THE HAMILTON-JACOBI EQUATION

Carter's original derivation [3] of the fourth invariant for the Kerr metric was performed by means of separation of the HJE for the Jacobi function S,

$$\dot{S} = \frac{1}{2} g^{\mu\nu} \frac{\partial S}{\partial q^\mu} \frac{\partial S}{\partial q^\nu}. \tag{13}$$

The Jacobi function generates the canonical transformation to action-angle variables [12]. Once S is known, the problem of finding the full set of constants of motion is solved. One method of solution of (13), and the only one so far used in practice, is by means of separation of variables.

Lack of separation of variables, however, does not necessarily imply that the system is not integrable or the absence of Q. An example that does not have its origin in the vacuum field equations is the Fokas-Lagerstrom Hamiltonian [17]

$$H = \tfrac{1}{2}(p_x^2 + p_y^2) + (x^2 - y^2)^{-2/3}, \tag{14}$$

which admits an orbital invariant

$$Q = (p_x^2 - p_y^2)(x p_y - y p_x) - 4(x p_y + y p_x)(x^2 - y^2)^{-2/3}. \tag{15}$$

No separation of variables for the HJE associated with (14) has ever been found.

In the case of the SAV spacetimes, all metrics admitting a second-rank Killing tensor have separable HJEs [4,18] in some coordinate system. This feature will be considered in greater detail in paper III of this series [5] where I will catalog the coordinate systems where this occurs.

IV. TESTS FOR INTEGRABILITY

To my knowledge, there exist no conclusive algebraic tests for integrability for a given 2-DOF Hamiltonian H. Many of the difficulties in carrying out a test are summarized in [16] and some will be demonstrated later in this paper. Partial tests, such as the Painlevé test, can be carried out and all dynamical systems that pass this test have been found to be integrable. Failure to pass the Painlevé test, however, does not imply that a particular Hamiltonian will fail the test in another coordinate system.

The Zipoy-Voorhees metric [10,11] fails the Painlevé test in the same manner that the Fokas-Lagerstrom Hamiltonian expressed in the form (14) does. This fact is inconclusive since after a number of difficult transformations a formulation of the Fokas-Lagerstrom Hamiltonian was found that passes the Painlevé test [16].

Possibly the strongest indication that integrability fails is the finding that numerical integration yields a Poincaré map without closed curves. A Poincaré map that displays closed curves is indicative that the Hamiltonian may be integrable, but it does not provide proof of the existence of an additional constant of motion.

If a Hamiltonian H is close to an integrable Hamiltonian H_0 with invariant Q_0, it is always possible, following a perturbative scheme developed by Deprit [19], to compute an approximate invariant Q associated with H, and thus to produce an approximate Poincaré map with closed curves. A perturbative invariant so constructed, however, may not give an accurate rendition of the phase space of the perturbed Hamiltonian H in a strongly chaotic regime. The classical example where this is clearly illustrated is the Hénon-Heiles problem [20]. A perturbative analysis is not sufficient to prove or disprove integrability.

Attempting to use the Deprit scheme of canonical perturbation theory to construct invariants for SAV spacetimes is prohibitively expensive computationally, and is not feasible if a solution for all SAV spacetimes is sought.

Indications of integrability can also be gleaned by observing the structure of the orbits in configuration space. This will be discussed in greater detail in subsequent paragraphs.

In paper IV of this series [6] I will propose a test to see if SAV spacetimes admit invariants that are polynomial in momenta.

V. ORBITS, PHASE SPACE, AND ENERGY SPACE

Integrable systems have a surprisingly simple structure [14]. If expressed in terms of action-angle variables, the orbits are found to trace out tori in the four-dimensional phase space (ρ, z, p_ρ, p_z). Although four dimensions are difficult to visualize, it is possible to see what these orbits look like in the three-dimensional energy space by introducing a momentum phase angle θ such that

$$p_\rho = \sqrt{J}\cos\theta, \qquad p_z = \sqrt{J}\sin\theta. \tag{16}$$

Doing so explicitly imposes the Hamiltonian constraint (9), so the orbit can be visualized in (θ, ρ, z) energy space, as depicted in Fig. 3. Note that if the light blue lines in this figure are "squashed", i.e. projected down onto the (ρ, z) plane, a rotated version of Fig. 2 is obtained.

One method of characterizing a curve in the (ρ, z) plane (Fig. 2) that is independent of the parameterization of the curve is to compute its curvature κ. (The curvature of a curve is a measure of how rapidly the curve is moving away from its tangent line.)

The curvature of a curve parameterized by $(\rho(\tau), z(\tau))$ can be expressed as

$$\kappa(\tau) = \frac{\dot{z}\,\ddot{\rho} - \dot{\rho}\,\ddot{z}}{(\dot{\rho}^2 + \dot{z}^2)^{3/2}}. \tag{17}$$

Using the momentum phase angle θ, this simplifies to

$$\kappa = \tfrac{1}{2}(\sin\theta\,\partial_\rho(\ln J) - \cos\theta\,\partial_z(\ln J)). \tag{18}$$

There are special points along a curve at which the curvature stops changing, or reaches an extremum, namely, when $\dot{\kappa} = 0$. These points are indicated by means of a dark blue line in Fig. 2. The surfaces in energy space on which these extrema occur can be computed for any J (See Appendix A). The brown surfaces shown in Fig. 3 are the extreme curvature surfaces.

The rate of change of the phase angle along a particular geodesic can be calculated and expressed compactly in terms of the curvature as

$$\dot{\theta} = -\frac{\kappa\sqrt{J}}{V}, \quad \text{or} \quad \theta' = -\kappa\sqrt{J}. \tag{19}$$

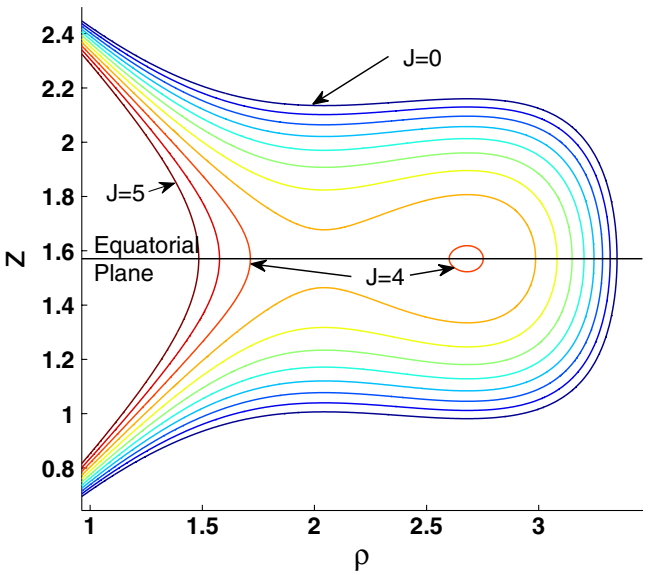

FIG. 1 (color online). Constant J potential surfaces for a geodesic in the Schwarzschild metric with $E = 0.95$, $L_z = 3$, $\mu = 1$. Contour Spacing 0.5. The explicit form of the metric functions can be found in Appendix C.

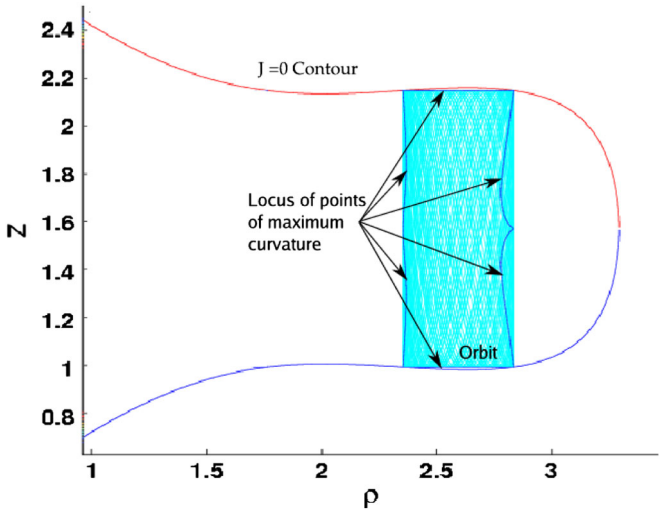

FIG. 2 (color online). Configuration (ρ, z) space depiction of a geodesic orbit for the potential J shown in Fig. 1 (Schwarzschild metric with $E = 0.95$, $L_z = 3$, $\mu = 1$).

If the geodesics are integrable, as is the case in Figs. 2 and 3, the orbits sweeps out a surface in the energy space (Fig. 3). The locus of points at which the orbit reaches a point of extreme curvature forms a curve in configuration space (Fig. 2). The points of contact with the $J = 0$ contour are unique, and are determined by the constant Q. Furthermore, if a Poincaré map is drawn it is constituted out of closed curves.

If the geodesic problem is not integrable (no Q exists) and the orbit is strongly chaotic, it will wander all over

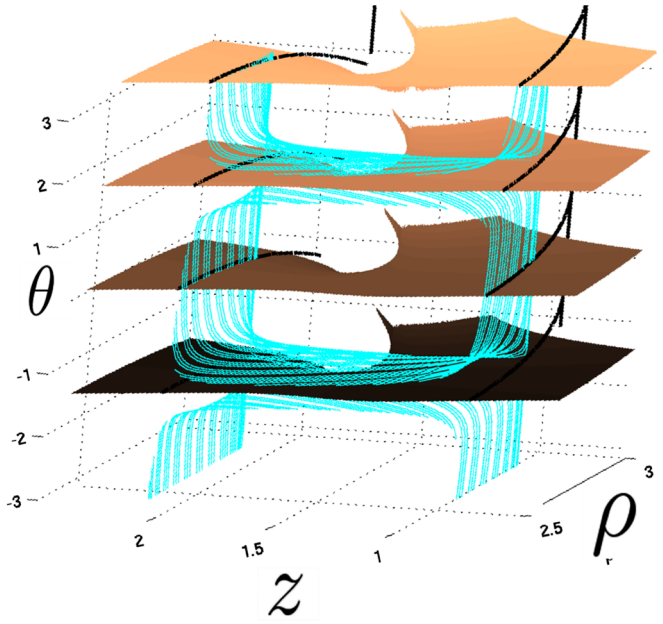

FIG. 3 (color online). Three-dimensional energy space depiction of the torus of the orbit displayed in Fig. 2. The orbit is depicted in cyan lines. The surfaces depicted correspond to the surfaces in phase space at which the orbit in configuration space reaches an extremum in curvature.

energy space. If the geodesic problem is not integrable and the Hamiltonian H is close to an integrable Hamiltonian H_0 the orbit can be confined to a small volume in phase space, and appear integrable. If both H and H_0 meet certain criteria [14], the manner in which the surfaces in energy space, or tori in configuration space, that exist for H_0 are destroyed are quantified by the Kolmogorov-Arnold-Moser (KAM) theorem [14].

VI. METHODS FOR CONSTRUCTING AN ADDITIONAL INVARIANT Q

Suppose now that you suspect that an additional invariant Q exists, due to a numerical exploration that yielded a Poincaré map with closed curves or due to the fact that the points of extreme curvature all lie on a curve or due to your Hamiltonian passing the Painlevé test; and suppose you would like to construct an explicit expression for Q. The rules of engagement to date appear to be simple: you guess its form and hope that you are right. One method of guessing is to postulate that the invariant Q is polynomial in momenta p. This is equivalent to guessing that you have a Killing tensor on your two manifold. This is by no means the only form an invariant can take; however most of the known examples of integrable two-dimensional Hamiltonians have polynomial Q's [16]. (For a further discussion on the generality of this form of guessing, see [21].)

The task of finding an additional invariant Q polynomial in momenta for a 2-DOF problem in dynamical systems has a long history. In some avenues of literature it is know as Whittaker's problem [14,22]. Hall [21] provides a very complete and readable reference and the analysis adopted here is guided largely by his treatment of the problem. This analysis will become particularly useful in paper IV [6] in this series when I return to a four-dimensional representation of the geodesic problem, and attempt to understand the coupling between the Weyl tensor of SAV spacetimes and the possible existence of Killing tensors. This method of analyzing the additional invariant appears to identify the most important quantities that should be considered, and provides a geometric picture of what they are. Some of the difficulties in checking why a given Hamiltonian is integrable are also illustrated. Furthermore, this approach highlights other properties an integrable orbit has. The problem was also considered by [16,23] and in different notation by [24–27].

Before I begin the analysis it is useful to introduce the complex variable $\zeta = 1/2(\rho + iz)$. Let $\bar{\zeta} = 1/2(\rho - iz)$ denote its complex conjugate. In terms of this complex variable the orbital curvature in the (ρ, z) plane can be expressed as

$$\kappa = \frac{1}{4i}(e^{i\theta}\partial_\zeta - e^{-i\theta}\partial_{\bar{\zeta}})\ln J, \tag{20}$$

and derivatives along the geodesic parameterized by λ

become

$$\partial_\lambda = p_\rho \partial_\rho + p_z \partial_z = \frac{\sqrt{J}}{2}(e^{i\theta}\partial_\zeta + e^{-i\theta}\partial_{\bar{\zeta}}). \tag{21}$$

Let us exploit the phase angle introduced in Eq. (16) to express our additional invariant Q, which is assumed to be a general Nth order polynomial in the momenta, p_ρ and p_z, as [cf. Equation (16)]

$$Q(\theta, \zeta, \bar{\zeta}) = \frac{1}{2}\sum_{n=-N}^{N} Q_n e^{in\theta}, \tag{22}$$

where the Q_n are complex valued functions of the configuration space variables, $Q_n = Q_n(\zeta, \bar{\zeta})$, n is a positive integer, and $Q_{-n} = \bar{Q}_n$. In effect, we are building up a Fourier series representation of the surface the orbit sweeps out in energy space; Fig. 3.

The condition that Q is invariant along the orbit, in other words that $Q' = 0$, results in differential equations for the functions Q_n. Explicitly, computing ∂_λ (22) and making use of $\theta' = -\kappa\sqrt{J}$ yields,

$$Q' = \frac{\sqrt{J}}{4}\sum_{n=-N}^{N} J^{n/2}\partial_\zeta(Q_n J^{-n/2})e^{i(n+1)\theta} + \frac{\sqrt{J}}{4}\sum_{n=-N}^{N} J^{-n/2}\partial_{\bar{\zeta}}(Q_n J^{n/2})e^{i(n-1)\theta}. \tag{23}$$

If this expression is to hold for all θ, the coefficients of $e^{ik\theta}$ must vanish for all $-(N+1) < k < (N+1)$, which translates into the conditions

$$\partial_\zeta\left(\frac{Q_n}{J^{n/2}}\right) = 0, \quad \text{for } n = N, N-1,$$
$$\partial_{\bar{\zeta}}(Q_{n+1}J^{(n+1/2)}) = -J^n\partial_\zeta\left(\frac{Q_{n-1}}{J^{((n-1)/2)}}\right), \quad \text{for } 0 < n \leq N-1, \tag{24}$$

where Q_0 is real and $\Re(\partial_{\bar{\zeta}}(Q_1\sqrt{J})) = 0$. For negative n values we get the complex conjugates of the above expressions. These equations can be identified directly with the Killing equations for a two manifold. The correspondence is shown in detail in Appendix B. The lessons learned here will be exploited in that setting in my paper IV [6].

Just as in a Fourier decomposition, the equations for odd and even n decouple. Furthermore, the first condition of (24) implies that

$$\frac{Q_N}{\sqrt{J}N} \equiv q_N(\bar{\zeta}) \tag{25}$$

is an analytic function of $\bar{\zeta}$ and indicates an inherent "gauge" freedom in the Killing equations. It is this freedom that makes the identification of integrable 2-DOF Hamiltonians so difficult. The integrability conditions that the functions Q_n exist result in conditions on the conformal factor J. As a result, you can write down the differential equations the conformal factor J must obey if it is to admit a Killing tensor in some coordinate system. However, if you are given a sample Hamiltonian to check for integrability, you have no idea what transformation leads to the coordinate system where we can conduct the check. An additional difficulty is that the conditions on the conformal factor for $N > 2$ are highly nonlinear.

In the case of SAV spacetimes that admits a second-rank Killing tensor (Carter spacetimes) it is possible to exploit the coordinate freedom to our advantage by coupling it to the gauge freedom in the metric [The R function in Eq. (1)]. A derivation of Carter spacetimes using this method is given in paper III of this series [5].

The case where $N = 1$, i.e. where the invariant Q is linear in the momenta, corresponds to a two metric with conformal factor J that admits a Killing vector. This implies that it is a manifold of constant curvature (of the two manifold, not the orbit). The curvature of the two manifold is given by

$$K = \tfrac{1}{2}\partial_{\zeta\bar{\zeta}}(\ln J). \tag{26}$$

The three possibilities include flat space ($K = 0$), the two sphere ($K > 0$), and the Lobachevskii plane ($K < 0$) which can be visualized as the surface of a bugle.

The problem of an invariant quadratic in the momenta ($N = 2$), on a two manifold was solved by Koenigs [26] in 1889, who distinguished four types that are closely related to the four separable coordinate systems found by Carter (a derivation is given in paper III [5]) and to the superintegrable systems studied by Kalnins *et al* [24,25]. The algebraic properties of two manifolds of this type are classified in [24,25]. Koenigs provided a very accurate geometric description of what the second quadratic invariant actually represents. This geometric picture was revisited and generalized by Moser [28], and clearly illustrated by Knörrer [29] in his study of geodesic flow on an ellipsoid. The second invariant corresponds to the Hamiltonian constant on a two manifold distinct from the first and there exists a very simple geometric construction mapping the geodesics on the one manifold to the next.

For the $N = 4$ case, very few examples are known [16,30]. It is my thesis that a large class of these two manifolds are generated by SAV spacetimes. I further suggest that the quartic structure is very closely related to the algebraic structure of the Weyl tensor, and that solution generation techniques for two manifolds already exist in the form of the solution generation techniques for SAV spacetimes. A test to see whether the SAV spacetimes admit a fourth order Killing tensor is proposed in paper IV of this series [6]. Numerical evidence that indicates that SAV spacetimes might generate two manifolds with fourth order Killing tensor is given in Sec. VII.

VII. NUMERICAL EXPERIMENTS AND ORBITAL STRUCTURE

The existence of an invariant Q of the form of Eq. (22), equivalently a Killing tensor, has direct implications for the orbital appearance of a geodesic. Consider a specific point in configuration space, for example, a point in Fig. 4, and consider the possible tangent directions that the geodesic could have leaving that point. The invariant Q restricts the possible exiting tangent directions to the number of zeros of Eq. (22).

To see this explicitly for the $N = 4$ case, consider a specific point P along an orbit characterized by the coordinates (ρ_P, z_P) in configuration space as displayed in Fig. 4. Suppose that the orbit admits an invariant of the form given in Eq. (22) and that Q denotes the constant along the orbit. Writing out Eq. (22) in terms of real quantities, and recalling that odd and even terms decouple, it becomes,

$$K_4^C \cos 4\theta + K_4^S \sin 4\theta + K_2^C \cos 2\theta + K_2^S \sin 2\theta + K_0 = 0, \tag{27}$$

where for a specific point P the constants K_0, K_i^C, and K_i^S are defined in terms of the series coefficients Q_n that enter Eq. (22) as $K_0 = Q_0 - 2Q$, $K_i^C = Q_i + \bar{Q}_i$, and $K_i^S = i(Q_i - \bar{Q}_i)$. The angle, θ, or tangent direction along which the orbit leaves point P is fixed using Eq. (27) to a number of discrete possibilities. In the $N = 4$ case, the oscillatory nature of Eq. (27) dictates that at most 8 values $\theta_k \in [0, 2\pi)$ can be found that lead to a solution. If in addition, the orbit can be traversed both ways, as in the SAV case, another constraint is introduced. Namely, that Eq. (27) should also hold if $\theta \to \pi - \theta$. The number of allowed exit directions from point P is halved. As a result, only 4 possible crossing directions (two crossing curves) are allowed at each point. This argument holds for every point P along the orbit. Orbits admitting a fourth order invariant thus display a very ordered, crosshatched appearance seen in Figs. 4 and 6 (region B). Many numerically explored SAV spacetimes display this crosshatching pattern.

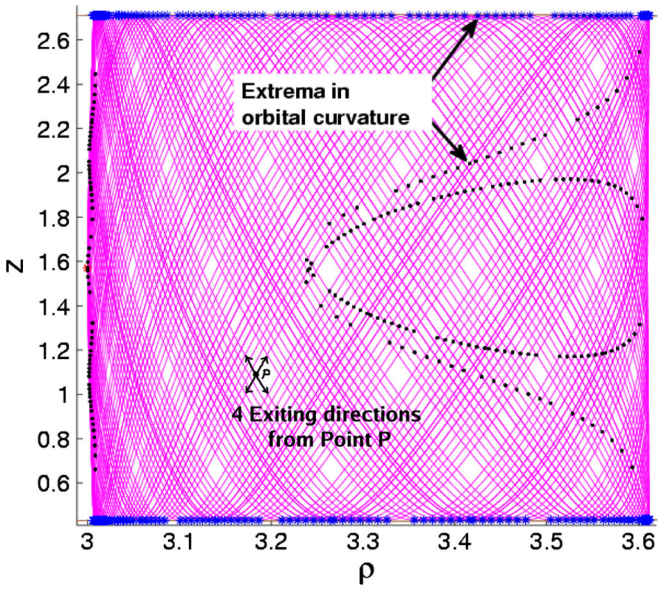

FIG. 4 (color online). An orbit in the Zipoy-Voorhees metric with $\delta = 2$. Orbital parameters are $E = 0.95$, $L = 3$, $\mu = 1$. The black dots and blue stars indicate extrema in orbital curvature.

In the preceding sentence, the meaning of the word "many" is intentionally vague and may best be interpreted as "surprisingly many". Surprising enough to warrant a more in depth exploration into the cause of the phenomenon. In mathematical terms, the number of SAV spacetimes explored numerically amounts to almost nothing, a set of measure zero. A careful accounting of the spacetimes explored as opposed to those available for exploration merely serves to underscore the absurdity of trying to quantify the geodesic nature of SAV spacetimes numerically. Furthermore, it gives a flavor of the *ad hoc* approach adopted thus far in this and other numerical explorations. Consider the class of all SAV spacetimes, each spacetime can be represented by a bi-infinite series of mass and spin multipole moments [31,32]. For a particular spacetime, different sets of orbital constants E, L_z, and μ are associated with one or more regions that admit a two metric J. Given a particular J the numerical exploration can proceed for individual orbits via, for example, Poincaré maps, or by observing its extreme curvature points, orbital structure, etc. In addition to the large number of parameters already mentioned, the freedom to choose the initial positions within the allowed two-dimensional region as well as the initial tangent direction still remains. The approach adopted numerically was to go looking for trouble in the form of chaotic, nonintegrable behavior. Orbital constants were chosen so that the orbit was near the strong-field region of the spacetime. For the resulting two metric J, initial conditions were randomly chosen. Of the bi-infinite parameterized class of available spacetimes, no more than 5 parameters were adjusted off their Kerr values, however, for a given parameter such as the quadrupole moment a large range of values were explored. It was the subjective impression that trouble was hard to find when compared to other well-known 2-DOF systems [20] explored by the author that sparked the original investigation into the problem. Integrable systems are rare, a set of measure zero. Consequently, repeatedly observing orbital behavior similar to that displayed in Fig. 4 and 6 (region B) albeit with slightly distorted potentials and angles in the crosshatching patterns was an unexpected surprise. The examples singled out in the following paragraphs are generic of the behavior observed to date. This does not preclude the possibility of getting into trouble and observing chaotic behavior upon more rigorous investigation. Ultimately, for precise statements to be made with respect to all SAV spacetimes or even to quantify with certainty the geodesic behavior of a

single spacetime that is not of type D, an algebraic check is required.

One example for which this crosshatched orbital structure is observed for all parameter values I explored, is the Zipoy-Voorhees metric [10,11]. A special case of the Weyl class, this metric has the multipole structure of a finite rod. The metric functions are given explicitly in Appendix D. It represents the one parameter (δ) family of spacetimes that links flat space ($\delta = 0$) to the Schwarzschild solution ($\delta = 1$). The orbital structure is displayed in Fig. 4.

An example of possibly greater astrophysical application in the EMRI problem is the Manko-Novikov spacetime [7–9] whose metric components are given in Appendix C. This parameterized metric allows one to explicitly adjust all the mass multipole moments as well as the spin of the central object. The initial exploration into the orbits of this spacetime was performed by Gair *et al.* [33], and unusual orbital behavior was observed.

Some of the properties of the Manko-Novikov spacetime are sketched in Fig. 10 and the functional form of the metric functions given in Appendix C. Figure 5 characterizes the nature of the metric functions close to the horizon.

In large regions of the parameter space of this spacetime, for example, region B of Fig. 6, the geodesic orbits display the characteristic fourth order crossing structure. There are, however, regions discovered by Gair *et al.* [33], where integrability fails and the orbit is chaotic. One such region in which chaos occurs is displayed in Fig. 6, region A. The inset provides the contours of the potential function J_A for this region; it lies outside the ergoregions displayed in Fig. 5. The Poincaré maps for this orbit fail to display closed curves [33] and the random orbital crossing structure implies that a Killing tensor on this manifold will never be found. I know of no similar example, in the literature of 2-DOF dynamical systems, where the orbits appear entirely integrable in one region and chaotic in another.

The numerical experiments conducted by Gair *et al.* [33] lead them to conclude that inspiralling orbits are unlikely to sample the ''chaotic'' region, so the possibility of observing such orbital behavior during a gravitational wave inspiral event is small, a conclusion with which I concur. However, conventional wisdom holds that if one observes the failure of integrability in some region of phase space it should preclude the construction of an invariant for the Hamiltonian in another. It would be an unfortunate and strange irony if chaotic behavior in a region of phase space that is observationally inaccessible prevents us from obtaining an explicit expression for an invariant in the region of phase space from which observable gravitational radiation results. It is this quantity that will give us theoretical power in describing inspiralling orbits in an algorithm for mapping spacetime.

Since the two regions A and B are disjoint, they can be considered as two separate two manifolds J_A and J_B, and

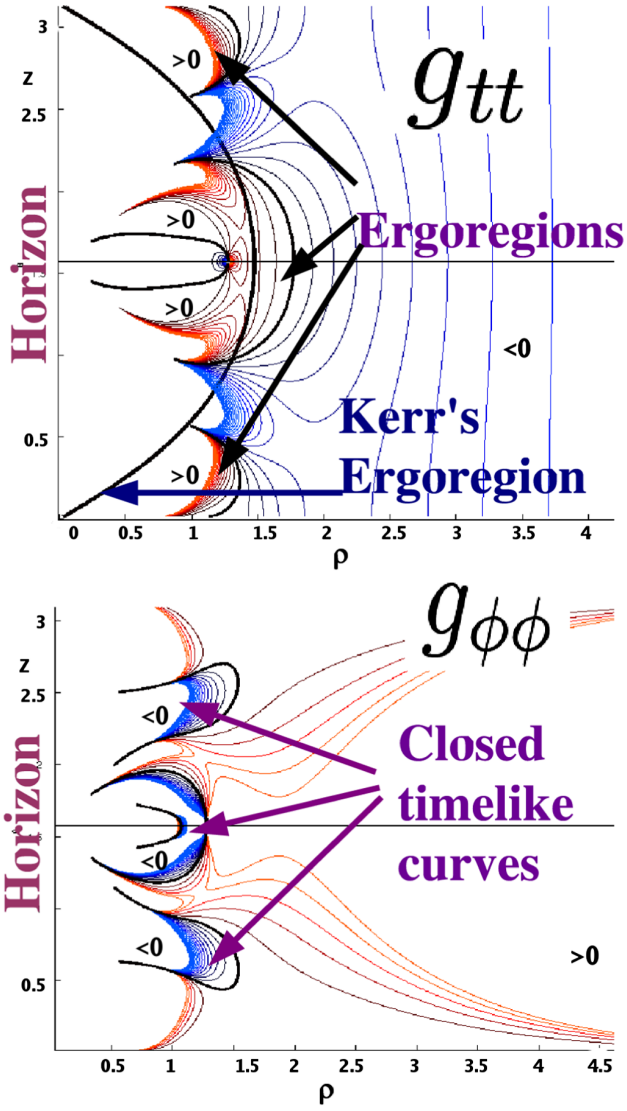

FIG. 5 (color online). Metric components of the Manko-Novikov spacetime. Thick black contours indicate zero values, red contours or regions marked by >0 admit positive values, and blue contours or <0, negative values.

following the analysis performed in this paper there is nothing that implies the chaos observed in region A precludes the existence of a Killing tensor on the two manifold J_B. To date the origin of the chaos in region A has not been carefully characterized. It is unclear whether the KAM theorem can be applied to this case, as the region A has no counterpart in the integrable Kerr spacetime, to which it reverts if the anomalous multipole moments are set to zero. In many ways the explanation of the orbital behavior in region A remains a very interesting puzzle.

VIII. CONCLUSION

This paper formulates the problem of finding the fourth invariant, more precisely, the generalization of Carter's constant to all SAV spacetimes, as a 2-DOF problem in

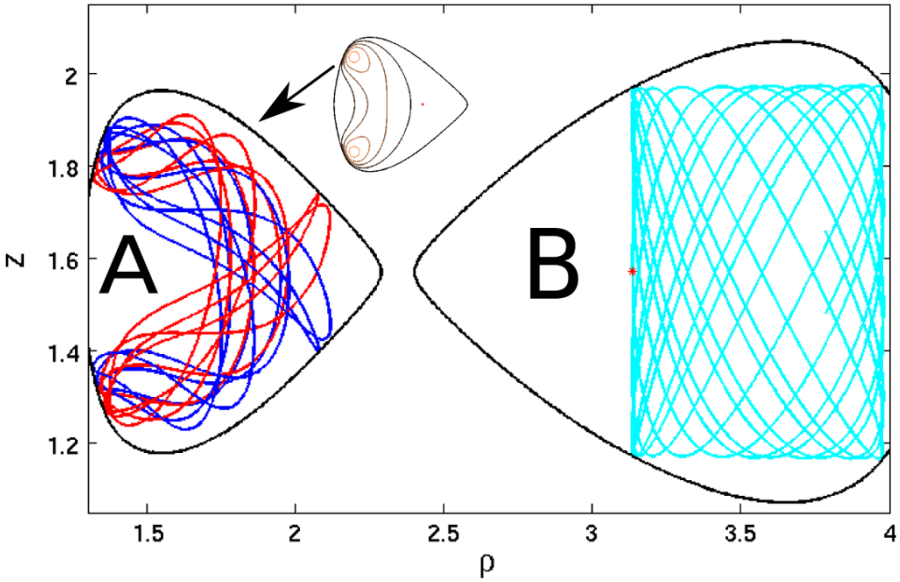

FIG. 6 (color online). Two orbits in the Manko-Novikov spacetime. The metric functions for this spacetime are given at the end of Appendix C, and the following parameters were used: $\alpha = 0.626789$, $\alpha_2 = 11.4708$, and $k = (1 - \alpha^2)/(1 + \alpha^2)$. The orbital parameters associated with the orbit in the figure are $E = 9.5$, $L = -3$, and $\mu = 1$.

dynamical systems. Equivalently stated, the problem can be formulated as the study of geodesic flow on a two manifold admitting a two metric with conformal factor J. A combination of the original metric functions in Eq. (1) and the constants that can be easily obtained from the metric symmetries determine J [Eq. (9)]. I summarize some related developments in dynamical systems and in the study of two manifolds, which may help this problem and point out some of the difficulties faced. In particular, I emphasize the absence of a conclusive algebraic check of whether a two manifold is integrable (or more specifically, possibly admits a Killing tensor), and the absence of a constructive method to construct invariants.

The two manifold approach to the problem has the great benefit that one can visually characterize the orbits and identify the possibility of integrable behavior. It further allows one to illustrate the geometric meaning of a Killing tensor. One problem faced during calculations is that the conformal factor J is very complicated, making the complete characterization of spacetimes for a given metric a formidable task and the characterization of all SAV spacetimes nearly impossible, using this approach.

A large class of SAV spacetimes have orbits that appear numerically to admit a fourth order invariant. This fact and the possibility of direct observational application if it does (paper I of this series [2]), has motivated a more in depth study (paper IV [6]). It turns out that in the context of the SAV spacetimes it may be possible to formulate an algebraic check that will determine whether a particular spacetime admits a higher order Killing tensor and thus quantify the relationship between the nonlocal metric distortion on a SAV spacetime described by the Weyl tensor and the dynamical behavior of particle motion within the spacetime. This formulation, however, requires the full power of the tetrad formalism and the solution generation techniques, which I will review in paper IV [6].

ACKNOWLEDGMENTS

I would like to thank Frank Estabrook from whom I learnt a great deal. I would also like to thank Ilya Mandel, Yasushi Mino, Kip Thorne, and Michele Vallisneri for many useful discussions and good advice.

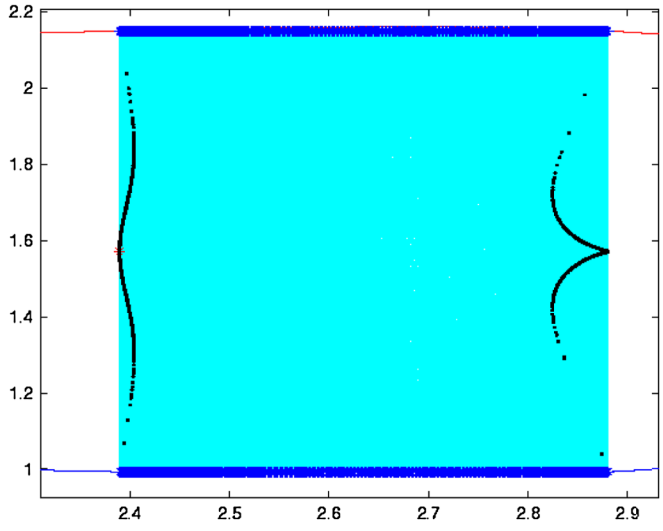

FIG. 7 (color online). Points of extreme orbital curvature in Schwarzschild $E = 0.95$, $L = 3$, $\mu = 1$. Black dots correspond to $n = \pm 1$ surfaces. Blue stars have $n = 0, 2$ in Eq. (A3).

APPENDIX A: SURFACES OF EXTREME ORBITAL CURVATURE

Points where an extremum of orbital curvature is reached can be computed by setting $\dot{\kappa}(\tau) = 0$. The points at which extrema in orbital curvature are reached, are shown in Figs.4 and 7 for an orbit in the Zipoy-Voorhees and Schwarzschild backgrounds, respectively. After some algebra one obtains

$$\dot{\kappa} = [\kappa, H] = \frac{1}{2VJ^{3/2}}(a(\cos^2\theta - \sin^2\theta) + 2b\cos\theta\sin\theta), \tag{A1}$$

where a and b are functions of (μ^2, E, L, ρ, z) defined as follows:

$$\begin{aligned} a &= \tfrac{3}{2}\partial_\rho J\partial_z J - J\partial_{\rho z}J, \\ b &= \tfrac{1}{2}J(\partial_{\rho\rho} - \partial_{zz})J - \tfrac{3}{4}((\partial_\rho J)^2 - (\partial_z J)^2). \end{aligned} \tag{A2}$$

As a result, curves in configuration space on which an extremum in curvature is reached ($\dot{\kappa} = 0$) can be parameterized by the phase angle θ_c at the point where

$$\theta_c = \frac{1}{2}\arctan\left(-\frac{a}{b}\right) + n\frac{\pi}{2}, \qquad n = \pm 0, 1, 2. \tag{A3}$$

The function $\theta_c(\rho, z, E, L, \mu^2)$ has four possible solution surfaces with $\theta_c \in (-\pi, \pi]$ (depicted in Fig. 8) This function can be thought of as a phase angle surface on which all points of extremal curvature must fall.

For each surface a branch cut occurs if $b = 0$. Curves of extreme orbital curvature provide an accurate way of quantifying where, given a particular J, a particular orbit will be confined in configuration space. In effect, what is constructed is a coordinate system ideally suited to the orbits. In Fig. 9, the extreme orbital curvature lines for several orbits for the J given in Fig. 2 are computed and the four points of contact with the $J = 0$ contour shown. Orbits on the left, that are not bound by a four pointed box, plunge through the horizon.

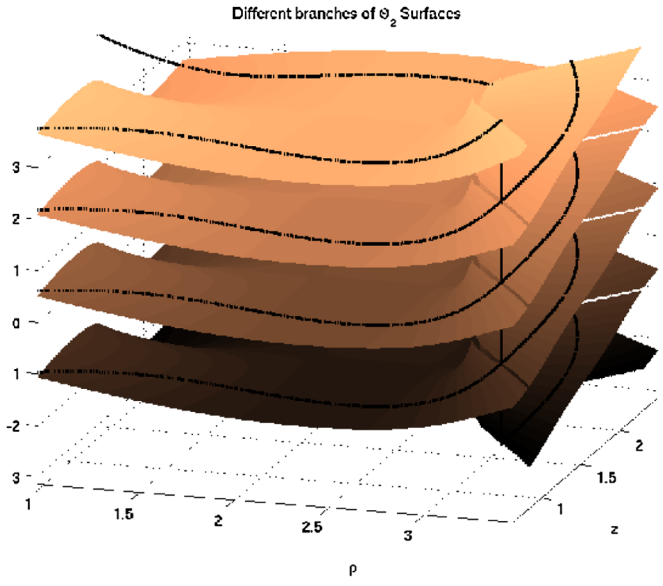

FIG. 8 (color online). The four branches on which solution points with extremal curvature can lie θ_c phase $E = 0.95$, $L = 3$, $\mu = -1$.

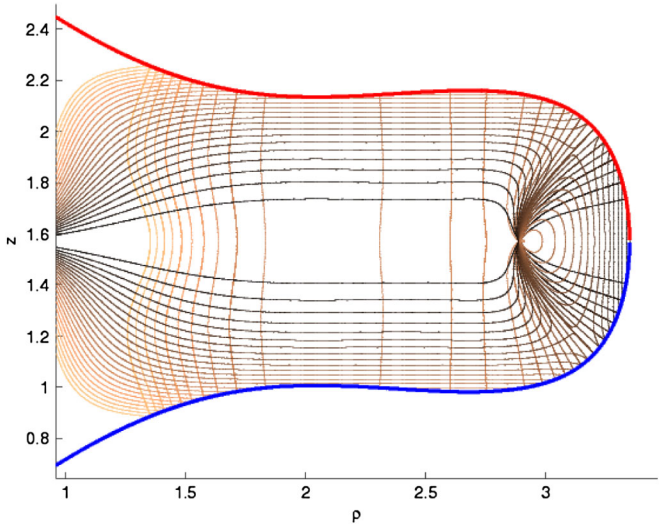

FIG. 9 (color online). Lines of extreme orbital curvature for several orbits of a given J. Schwarzschild $E = 0.95$, $L_z = 3$, $\mu = 1$.

Many quantities associated with the curvature and with extreme curvature surfaces can be most compactly expressed in complex notation. Introduce the complex variable $\zeta = 1/2(\rho + iz)$ and the complex function $c = b + ia$. Using Eq. (A2), c can be expressed in terms of the potential J as follows

$$c = \frac{1}{2}J\partial_{\zeta\zeta}J - \frac{3}{4}(\partial_\zeta J)^2 = -J^{5/2}\partial_{\zeta\zeta}\left(\frac{1}{\sqrt{J}}\right), \tag{A4}$$

and the extreme curvature conditions is

$$e^{i2\theta_c}c - e^{-2i\theta_c}\bar{c} = 0. \tag{A5}$$

APPENDIX B: KILLING TENSORS IN 2D

The correspondence between the components of a phase space expansion Q_n for calculating the invariant Q [Eq. (22)] and polynomial in momenta and components of a Killing tensor on the two manifold is given.

Consider the two metric $g_{J_{ij}} = J\delta_{ij}$ on a two manifold admitting a totally symmetric Killing tensor $T^{(\alpha_1\cdots\alpha_N)}$ of order N.

The Killing equations

$$T^{(\alpha_1\cdots\alpha_N)}{}_{;b} = 0, \tag{B1}$$

imply that

$$Q_T = T^{(\alpha_1\cdots\alpha_N)}p_{\alpha_1}\cdots p_{\alpha_N} \tag{B2}$$

remains constant along the geodesic. Making use of the definition of the momentum phase angle, Eq. (16), the invariant Q_T can be rewritten as

$$Q_T = J^{N/2} T^{(\alpha_1 \cdots \alpha_N)} \prod_{i=1}^{N} \cos\left(\theta + \frac{(1-\alpha_i)\pi}{2}\right), \tag{B3}$$

where $\alpha_i = 1$ indicates the index ρ and $\alpha_j = 2$ the index z. To put this in the form of Eq. (22), let $P_{(n,N)}(i, j)$ denote the jth entry of the ith permutation of a list of a total of N elements containing $N - n$ entries equal to 1 and n entries equal to -1. Let $p(n)$ denote the number of permutations. As an example of the notation, let $N = 4$. Then $P_{(0,4)}(1, j) = (1, 1, 1, 1)$ has one permutation, $P_{(1,4)}$ has 4 permutations, and $P_{(2,4)}$ has 6; these are explicitly listed as follows:

$$\begin{aligned}
&P_{(1,4)}(1,j) = (-1,1,1,1), \quad P_{(1,4)}(2,j) = (1,-1,1,1),\\
&P_{(1,4)}(3,j) = (1,1,-1,1), \quad P_{(1,4)}(4,j) = (1,1,1,-1),\\
&P_{(2,4)}(1,j) = (-1,-1,1,1), \quad P_{(2,4)}(2,j) = (-1,1,-1,1),\\
&P_{(2,4)}(3,j) = (-1,1,1,-1), \quad P_{(2,4)}(4,j) = (1,-1,-1,1),\\
&P_{(2,4)}(5,j) = (1,-1,1,-1), \quad P_{(2,4)}(6,j) = (1,1,-1,-1).
\end{aligned} \tag{B4}$$

For clarity assume N is even. (The result also holds for odd N but more care has to be taken with the index ranges.) The product of cosines can then be expressed as

$$\prod_{i=1}^{N} \cos(\theta + \beta_i) = \frac{1}{2^N} \sum_{l=-N/2}^{N/2} \sum_{k=1}^{p(N-2l/2)} e^{2il\theta} \times \exp\left(\sum_{j=1}^{N} i\beta_j P_{((N-2l/2),N)}(k, j)\right). \tag{B5}$$

Thus the correspondence between the even terms in the series for even N and the Killing tensor components is

$$Q_{2l} = 2\frac{J^{N/2}}{2^N} T^{(\alpha_1 \cdots \alpha_N)} \sum_{k=1}^{p(N-2l/2)} i^{(\Sigma_{j=1}^{N}(1-\alpha_j)P_{((N-2l/2),N)}(k,j))}. \tag{B6}$$

In the case where $N = 2l$, the analytic function, mentioned in Eq. (25), is

$$q_N(\bar{\zeta}) = \frac{Q_N}{\sqrt{J^N}} = 2\frac{1}{2^N} T^{(\alpha_1 \cdots \alpha_N)} i^{(\Sigma_{j=1}^{N}(1-\alpha_j))}. \tag{B7}$$

The explicit expressions for the analytic function and Q_0 term of the lowest order case $N = 2$ are

$$q_2 = \tfrac{1}{2}(T^{\rho\rho} - T^{zz} - 2iT^{\rho z}), \qquad Q_0 = J(T^{\rho\rho} + T^{zz}). \tag{B8}$$

For the $N = 4$ case the expansion terms Q_n expressed as a sum of the fourth order Killing tensor components are

$$\begin{aligned}
q_4 &= \frac{1}{8}(T^{\rho\rho\rho\rho} + T^{zzzz} - 6T^{zz\rho\rho} + 4i(T^{\rho\rho\rho z} - T^{\rho zzz})),\\
Q_2 &= \frac{J^2}{2}(T^{\rho\rho\rho\rho} - T^{zzzz} - 2i(T^{\rho\rho\rho z} + T^{\rho zzz})),\\
Q_0 &= \frac{3J^2}{4}(T^{\rho\rho\rho\rho} + 2T^{zz\rho\rho} + T^{zzzz}).
\end{aligned} \tag{B9}$$

APPENDIX C: MANKO-NOVIKOV METRIC

The metric of the Manko-Novikov spacetime [7] used to generate the plots in Figs. 5 and 6 and whose properties are sketched in Fig. 10, can be generated from the Ernst potential of the form $\mathcal{E} = e^{2\tilde{\psi}} A_-/A_+$ where

$$\begin{aligned}
&A_\mp = x(1 + ab) + iy(b - a) \mp (1 - ia)(1 - ib),\\
&\Delta\tilde{\psi} = 0,
\end{aligned} \tag{C1}$$

and the coordinates $x = \cosh\rho$ and $y = \cos z$ are called the Weyl coordinates. The metric functions that enter Eq. (1) are

$$\begin{aligned}
R^2 &= k^2(x^2 - 1)(1 - y^2),\\
e^{2\gamma} &= e^{2\tilde{\gamma}} \frac{A(x^2 - y^2)}{(x^2 - 1)(1 - \alpha^2)^2},\\
e^{2\psi} &= e^{2\tilde{\psi}} \frac{A}{B},\\
\omega &= 2ke^{-2\tilde{\psi}} \frac{C}{A} - \frac{4k\alpha}{1 - \alpha^2},
\end{aligned} \tag{C2}$$

where

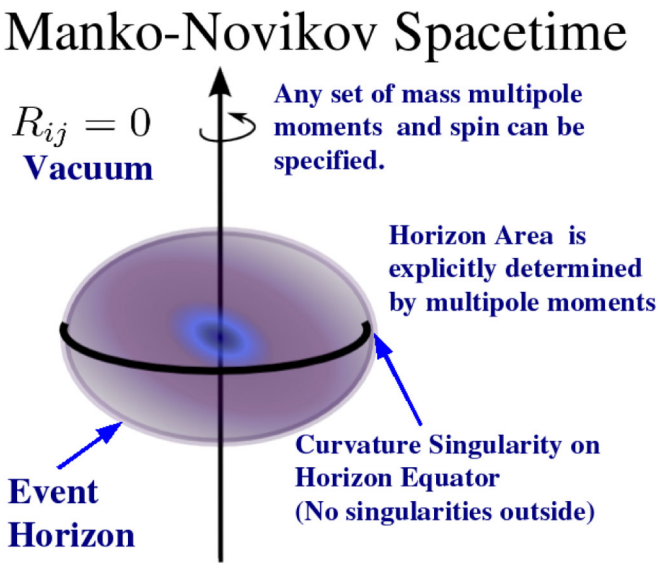

FIG. 10 (color online). Properties of the Manko-Novikov spacetime.

$$A = (x^2-1)(1+ab)^2 - (1-y^2)(b-a)^2,$$
$$B = [x+1+(x-1)ab]^2 + [(1+y)a+(1-y)b]^2,$$
$$C = (x^2-1)(1+ab)[b-a-y(a+b)] + (1-y^2)(b-a)[1+ab+x(1-ab)]. \quad \text{(C3)}$$

The functions a and b obey a set of differential equations stated in [7], and one example of a solution is given below.

The solution for which the plots are made is a quadrupolar spacetime. Let $r = (x^2+y^2-1)^{1/2}$ and $u = xy/r$, and define the required Legendre polynomials to be $P_0(u) = 1$, $P_1(u) = u$, $P_2(u) = -1/2 + (3/2)u^2$, and $P_3(u) = u(5u^2-3)/2$. Then

$$\ln\left(\frac{a}{-\alpha}\right) = -2\alpha_2\left[(x-y)\left(\frac{P_0}{r}+\frac{P_1}{r^2}+\frac{P_2}{r^3}-1\right)\right],$$
$$\ln\left(\frac{b}{\alpha}\right) = -2\alpha_2\left[(x+y)\left(\frac{P_0}{r}-\frac{P_1}{r^2}+\frac{P_2}{r^2}\right)-1\right],$$
$$\tilde{\psi} = \alpha_2\frac{P_2}{r^3},$$
$$\tilde{\gamma} = \frac{1}{2}\ln\frac{x^2-1}{x^2-y^2} - \frac{1}{2}\left(\ln\left(\frac{a}{-\alpha}\right)+\ln\left(\frac{b}{\alpha}\right)\right) + \alpha_2^2\left(\frac{3}{2}\right)^2\frac{P_3^2-P_2^2}{r^6}. \quad \text{(C4)}$$

Note that $\tilde{\psi}$ and $\tilde{\gamma}$ are members of the Weyl class of static metrics, α is a parameter that scales the spin, and α_2 is the quadrupole moment. The Geroch-Hanson multipole moments for this metric can be found in [7] along with a more general solution parameterized by arbitrary mass multipole moments. In the event that $\alpha = 0$ and $\alpha_2 = 0$, the metric reduces to the Schwarzschild metric with metric functions

$$e^{2\psi} = \left(\frac{x-1}{x+1}\right), \qquad e^{2\gamma} = \left(\frac{x^2-1}{x^2-y^2}\right), \qquad R^2 = (x^2-1)(1-y^2), \qquad \omega = 0, \qquad k = 1. \quad \text{(C5)}$$

APPENDIX D: ZIPOY-VOORHEES METRIC

The Zipoy-Voorhees metric [10,11] is a static spacetime with metric functions

$$e^{2\psi} = \left(\frac{x-1}{x+1}\right)^{\delta}, \qquad e^{2\gamma} = \left(\frac{x^2-1}{x^2-y^2}\right)^{\delta^2}, \qquad R^2 = (x^2-1)(1-y^2), \qquad \omega = 0, \qquad k = 1. \quad \text{(D1)}$$

All numerical experiments performed in this metric thus far appear to admit integrable orbits similar to that portrayed in Fig. 4.

[1] F. D. Ryan, Phys. Rev. D **52**, 5707 (1995).
[2] J. Brink, preceding Article, Phys. Rev. D **78**, 102001 (2008).
[3] B. Carter, Phys. Rev. **174**, 1559 (1968).
[4] B. Carter, Commun. Math. Phys. **10**, 208 (1968).
[5] J. Brink, "III. Second order Killing Tensors" (unpublished).
[6] J. Brink, "IV. Relationship between Weyl Curvature and Killing Tensors in SAV Spacetimes" (unpublished).
[7] V. S. Manko and I. D. Novikov, Classical Quantum Gravity **9**, 2477 (1992).
[8] J. Castejon-Amenedo and V. S. Manko, Phys. Rev. D **41**, 2018 (1990).
[9] V. Manko, Classical Quantum Gravity **7**, L209 (1990).
[10] B. Voorhees, Phys. Rev. D **2**, 2119 (1970).
[11] D. M. Zipoy, J. Math. Phys. (N.Y.) **7**, 1137 (1966).
[12] H. Goldstein, *Classical Mechanics* (Addison-Wesley Publishing Company, Reading, MA, 1980), ISBN 0-201-02918-9.
[13] R. Abraham and J. E. Marsden, *Foundations of Mechanics* (The Benjamin/Cummings Publishing Company, Inc., Reading, MA, 1978).
[14] M. Tabor, *Chaos and Integrability in Nonlinear Dynamics—An Introduction* (John Wiley & Sons, New York, 1989), ISBN .
[15] S. H. Strogatz, *Nonlinear Dynamics and Chaos with Applications to Physics, Biology, Chemistry and Engineering* (Perseus Books , Reading, MA, 1994).
[16] J. Hietarinta, Phys. Rep. **147**, 87 (1987).
[17] A. S. Fokas and P. A. Lagerstrom, J. Math. Anal. Appl. **74**, 325 (1980).
[18] N. M. J. Woodhouse, Commun. Math. Phys. **44**, 9 (1975).
[19] A. Deprit, Celest. Mech. **1**, 12 (1969).
[20] M. Hénon and C. Heiles, Astron. J. **69**, 73 (1964).
[21] L. S. Hall, Physica D (Amsterdam) **8**, 90 (1983).
[22] E. Whittaker, *A Treatize on the Analytical Dynamics of Particles and Rigid Bodies* (Dover Publications, New York, 1944).
[23] B. C. Xanthopoulos, J. Phys. A **17**, 87 (1984).
[24] E. G. Kalnins, J. M. Kress, and P. Winternitz, J. Math. Phys. (N.Y.) **43**, 970 (2002).
[25] E. G. Kalnins, J. M. Kress, and W. Miller, J. Math. Phys. (N.Y.) **46**, 053509 (2005).
[26] G. Koenigs, Sur les Geodesiques a Integrales Quadratiques, in *Lecons sur la Theorie Generale des Surfaces*, edited by G. Darboux (Gauthier-Villars, Paris, 1894) (republished by Chelsea, New York, 1972), Vol. 4, p. 368.
[27] M. Walker and R. Penrose, Commun. Math. Phys. **18**, 265 (1970).
[28] J. Moser, in *The Chern Symposium: Proceedings of the International Symposium on Differential Geometry in*

Honor of S.-S. Chern, Berkeley, California, June 1979, (Springer, New York, 1979), p. 147.
[29] H. Knörrer, Inventiones Mathematicae **59**, 119 (1980).
[30] M. Karlovini, G. Pucacco, K. Rosquist, and L. Samuelsson, J. Math. Phys. (N.Y.) **43**, 4041 (2002).
[31] R. Geroch, J. Math. Phys. (N.Y.) **12**, 918 (1971).
[32] R. Geroch, J. Math. Phys. (N.Y.) **13**, 394 (1972).
[33] J. R. Gair, C. Li, and I. Mandel, Phys. Rev. D **77**, 024035 (2008).